

A Compact Novel Quad Patch High Gain Triple Band Microstrip Antenna for 5G/6G mm Wave Applications

R. K. Singh^{1*}, K. Mamta²

¹University Department of Physics, Ranchi University, Ranchi-834008, India

²Department of Physics, Nalanda College of Engineering, Chandi, Nalanda-803108, India

Received 7 June 2023, accepted in final revised form 8 November 2023

Abstract

This paper presents a compact, novel, quad patch and triple band single substrate microstrip patch antenna for 5G/6G mm wave applications. The aim is to design an antenna within the K-band with three resonance frequencies at 24, 29, and 34 GHz. The antenna is designed on a volumetric dimension of $11 \times 12.7 \times 1.6 \text{ mm}^3$. The substrate used is FR4 (dielectric constant 4.4), having a loss tangent of 0.0022. A microstrip line of width 1 mm for a 50Ω impedance line is used to match with the load antenna, which has four rectangular connected patches. Patch dimensions come from standard antenna equations and simulation done on Ansys High-Frequency Structure Simulator software. Validation of simulated results is done through measurements on the prototype antenna. A substantial good agreement is found between the simulated and measured results. The gain of the proposed antenna is 6.16 dBi, with return loss being $\leq -10 \text{ dB}$. Bandwidths are 1.1 GHz (23.8 - 24.9 GHz), 0.9 GHz (28.6 - 29.5 GHz), and 0.8 GHz (33.7 - 34.5 GHz), respectively. The far-field radiation characteristics of both E-plane and H-plane are also reported. The proposed design is suitable for mm wave applications, including smart vehicles, global positioning systems, radio frequency identifications, etc.

Keywords: Antenna Gain; Patch antennas; Return loss; Voltage standing wave ratio; Yagi-Uda antennas.

© 2024 JSR Publications. ISSN: 2070-0237 (Print); 2070-0245 (Online). All rights reserved.
doi: <http://dx.doi.org/10.3329/jsr.v16i1.66715> J. Sci. Res. **16** (1), 187-199 (2024)

1. Introduction

The demand for mobile communication systems has increased significantly during the past ten years and is still growing. GPS, Wi-MAX, and WLAN are the key standards in mobile communication. Effective small-size antennas are needed for these wireless applications. As cellular and mobile technologies have advanced, so has portable antenna technology [1-4]. A multiband antenna with pattern diversity can meet the unique requirements of the communication system for polarization and radiation direction in different frequency bands, in addition to supporting the operating frequency bands under multiple wireless system standards, significantly enhancing the antenna's functionality.

* Corresponding author: rajksingh08@gmail.com

However, the antenna's construction and associated operations are quite intricate, and radiation performance still needs to be enhanced.

Wireless systems have a strong need for antennas that are both small in size and have several bands. This is so they can support various functions in their antennas. Yet, creating a multiband antenna that is both compact and electrically efficient without compromising the antenna's performance is quite difficult [5-8].

Because of its ability to operate in various frequency bands, including DCS, Wi-Fi, WLAN bands (802.11 b/n/g), and WiMAX, multiband antennas are crucial for mobile communications (IEEE 802.16). These applications can employ a variety of antenna types, including PIFA, dipole, monopole, etc. The microstrip patch antenna (MPA), in general, is a crucial component of the communication system because it has several distinctive and attractive qualities. Some of these qualities are small size, low price, straightforward design, lightweight, simplicity of fabrication, and broad bandwidth. Microstrip antenna fits these requirements as it employs a millimeter wave frequency spectrum in the range of 1 to 10 mm [9-14].

The Yagi-Uda antenna is a traditional antenna that is frequently used in wireless communications due to its excellent directivity, simple form, ease of feeding, and inexpensive cost. Over the past few years, many improvements have been made to the Yagi-Uda antenna's design and optimization for certain applications. [15-18].

This paper proposes a compact novel microstrip quad patch tri-band Yagi-Uda-like antenna for 5G/6G mm Wave applications. Simple patch structures are used to achieve the tri-band performance. The proposed antenna is characterized by its simple structure, which is easy to fulfill at a low cost. The aim is to design an antenna with three resonance frequencies at 24, 29, and 34 GHz, with spacing of 5 GHz between each resonance frequency with VSWR < 2, which can satisfy the application requirements excellently.

2. Methodology

A microstrip patch antenna is a three-layer device. The top layer is a radiating patch, which is a metal foil. The bottom layer is the ground, and a dielectric substrate exists between the top and bottom layers. The radiation in the microstrip patch antenna is caused by the fringing fields. The microstrip antenna's radiation is created by the phase-added addition of the fringing E-fields on its border. In contrast to wire antennas, which radiate because the currents build up in phase and are, therefore, "current radiators," the patch antenna radiates because it is a "voltage radiator." The idea of patches has been explored by many researchers using different forms of patches and slots [19-28]. Free space propagation losses and penetration losses have been drastically reduced using mm wave bands of 5G technology [29-34]. Millimeter wave band-based antenna comes with certain embodied losses like dielectric loss, conductor loss, radiation loss, etc. Dielectric loss can be set with the use of a substrate of low-loss tangent. The low dielectric constant is linked with low total loss of the microstrip. Radiation loss becomes significant for thicker substrates as this comes with more surface current.

The proposed Yagi-Uda-shaped antenna is designed on a single-layered substrate, which corresponds to a volumetric size of $11 \times 12.7 \times 1.6 \text{ mm}^3$ (Fig. 1). The patch of the antenna was calculated based on the standard microstrip equation and the dimension was adjusted for optimization. Design equations for different parameters of the microstrip patch antenna are shown in Table 1.

Table 1. Design equations for different parameters of microstrip patch antenna.

Parameter	Design equation
Substrate height, h	$h \leq \frac{0.3 c}{2 * 3.14 f_r \sqrt{\epsilon_r}}$
Patch length, Lp	$Lp = \frac{c}{2 \sqrt{\epsilon_r^{eff}}} \left(\frac{1}{f_r} \right) - 2(\Delta L)$
Patch width, Wp	$Wp = \frac{c}{2 f_r} \sqrt{\frac{2}{\epsilon_r + 1}}$
Effective dielectric constant, ϵ_r^{eff}	$\epsilon_r^{eff} = \frac{1}{2}(\epsilon_r + 1) + \frac{1}{2}(\epsilon_r - 1) \left(1 + 12 \frac{h}{Wp} \right)^{-1/2}$
Length extension, ΔL	$\frac{\Delta L}{h} = 0.412 \frac{(\epsilon_r^{eff} + 0.3) \left(\frac{Wp}{h} + 0.264 \right)}{\left(\frac{Wp}{h} + 0.8 \right) (\epsilon_r^{eff} - 0.258)}$

Where ϵ_r = Dielectric constant of substrate, c = velocity of light in free space, f_r = resonant frequency

The radiating patch of the antenna is printed on substrate F4 (dielectric constant 4.4). A microstrip line of 50Ω impedance is used to match with the load antenna for supplying energy to the four radiating patches. A lumped port and an air radiation box are designed in this process. Dimensions of the antenna design are listed in Table 2.

Table 2. Antenna design dimensions.

Name	Length along X axis (mm)	Length along Y axis (mm)	Length along Z axis (mm)
Ground	11	12.7	-0.001
Substrate	11	12.7	1.6
Feed	5.6	1	
Port		1	-1.61
Radiation box	20	20	10
First Patch	1.5	3	
Second Patch	1.5	4	
Third Patch	1.5	6	
Fourth Patch	1.5	8	

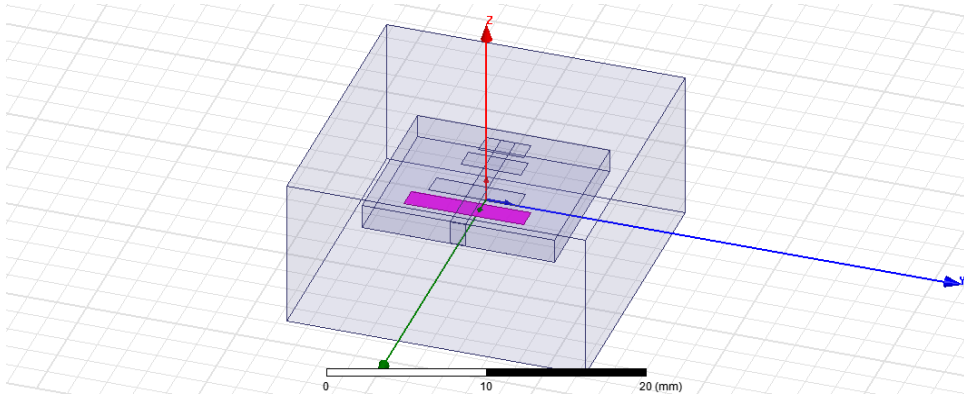


Fig. 1. Geometry of the proposed antenna design.

The antenna consists of the radiating element and the feed structure. The radiating element is obtained with four different size rectangular patches to achieve a wider bandwidth. Impedance matching of the antenna is done by tuning the size of patches in the feeding portion. This follows a prototype antenna fabrication based on the HFSS simulated results. The simulated bandwidth of the proposed antenna is about 4.7 % (23.8 - 24.9 GHz), 3.1 % (28.6 - 29.5 GHz), and 2.4 % (33.7 - 34.5 GHz) with $VSWR < 1.6$. The port isolation is better than 13 dB over the entire range of operating frequencies. Further, the proposed antenna has a stable gain of 6.16 dBi.

3. Result and Discussion

Results on the antenna parameters and their performances are reported separately as simulation results and measured results in this section. The comparison between the two results is also reported.

3.1. Simulation results

S11 measures the amount of energy returning back to the analyzer. It doesn't measure the energy delivered to the antenna. From Fig. 2, it is clear that the designed antenna radiates best at 24.8, 29.7, and 34 GHz, where S11 is below -10 dB. In and around these best-performing frequencies, S11 at 24.54 GHz is -13.05 dB, at 29.84 GHz, S11 is -13.15 dB, and at 34.39 GHz, the S11 is -12.73 dB.

The ratio of incident power to the reflected power in dB is the return loss, whereas the ratio of incident power to transmitted power in dB is the insertion loss. The return loss turns out to be -13 dB. This means that the transmitted signal will not be affected by reflected signals. Further, since the return loss is less than -10 dB, insertion loss will be almost nil.

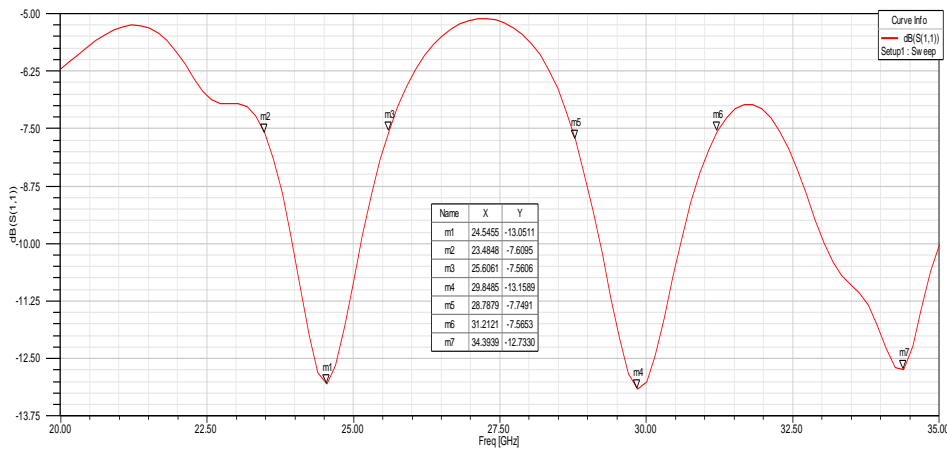


Fig. 2. S11 parameter. S11 at 24.54 GHz is -13.05 dB, at 29.84 GHz, S11 is -13.15 dB, and at 34.39 GHz, the S11 is -12.73 dB.

At Frequencies 24, 29, and 34 GHz, maximum power is realized by the patch, i.e., the best impedance matching happens between the feedline and patch.

Voltage Standing Wave Ratio (VSWR) gauges how well an antenna and the feed line it is connected to are matched. In an ideal system, 100% of the energy is transmitted. In real systems, mismatched impedances cause some of the power to be reflected back toward the source. A VSWR value under 2 is considered ideal and suitable for most antennae. In the proposed antenna, the graph shows, at 24.54, 29.9, and 34.39 GHz, the VSWR values of 1.57, 1.57, and 1.60, respectively, all as per the ideal requirement (Fig. 3).

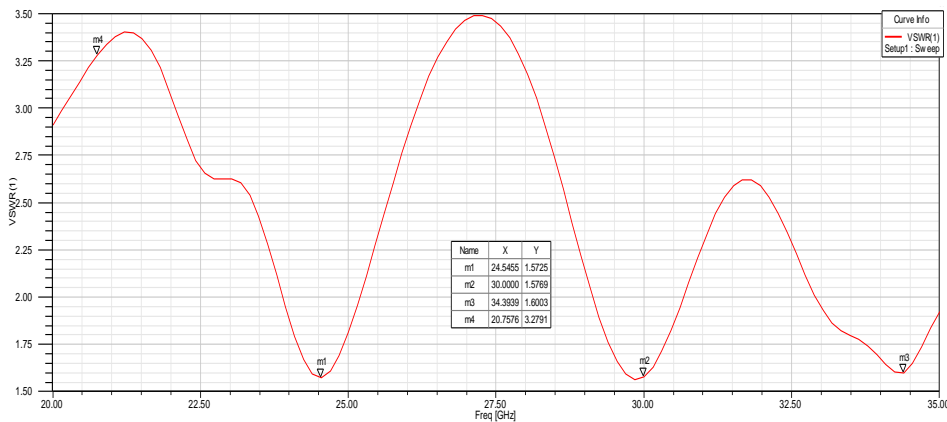


Fig. 3. VSWR: At 24.54, 29.9, and 34.39 GHz, the VSWR is 1.57, 1.57 and 1.60, respectively, which are less than 2, the ideal requirement.

The bandwidth of an antenna refers to the range of frequencies over which the antenna satisfies a particular parameter specification. The impedance bandwidth of the

proposed antenna is about 1.1 GHz (23.8 - 24.9 GHz), 0.9 GHz (28.6 - 29.5 GHz), and 0.8 GHz (33.7 – 34.5 GHz). The E-plane and three-dimensional radiation patterns are shown in Figs. 4 and 5, respectively.

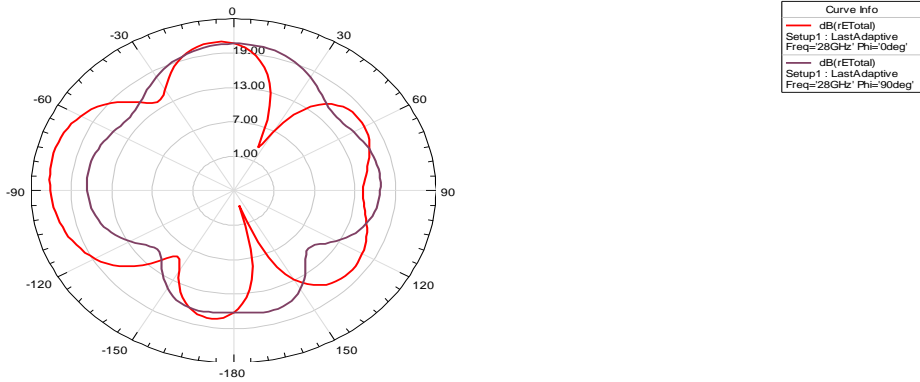


Fig. 4. E-plane radiation pattern for the four patches at frequency 28 GHz.

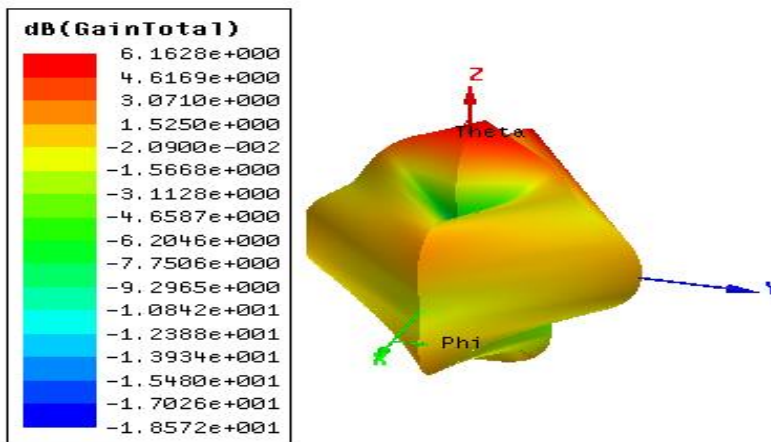


Fig. 5. Three-dimensional radiation pattern.

Antenna gain is the ability of the antenna to radiate more or less in any direction compared to a theoretical antenna. Antenna gain is the measure of antenna power in decibels (dB), which is equal to $10 \cdot \log(P_{out}/P_{in})$. High-gain antennas allow longer range in one direction but need to be pointed accurately. Low-gain antennas have a lower range but can receive signals from a wider span of direction. The proposed antenna has a 6.16 dB gain (Fig. 6) at a frequency of 34 GHz, which is a very acceptable value because this will offer a good range balance and will be able to connect to nearby antennas at different heights with a coverage of around 350. Gains at frequencies 24 and 29 GHz are -1.0 and -1.5 dB, respectively.

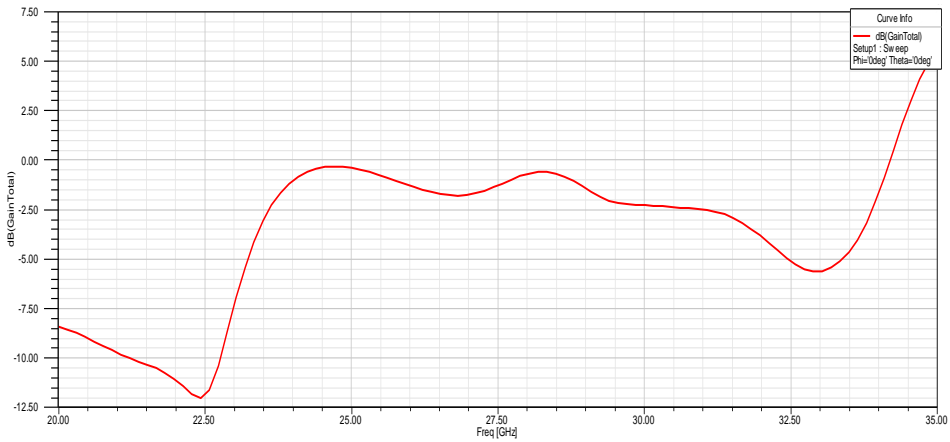


Fig. 6. Gain versus frequency. A gain of 6.16 dB is obtained, offering a good coverage of approximately 35°.

Admittance is a gauge of how easily a device or circuit will let a current pass. It is described as an impedance's reciprocal. Admission is a complex integer with two components: an imaginary susceptance (B) and a real conductance (G). A good conductance values viz. 0.5385 and 0.8729 are obtained from the real Y plot against frequency at the desired operational frequencies (Fig. 7). A susceptance of -0.0318 around the frequency 27 GHz is good enough for the practicability of the antenna (Fig. 8).

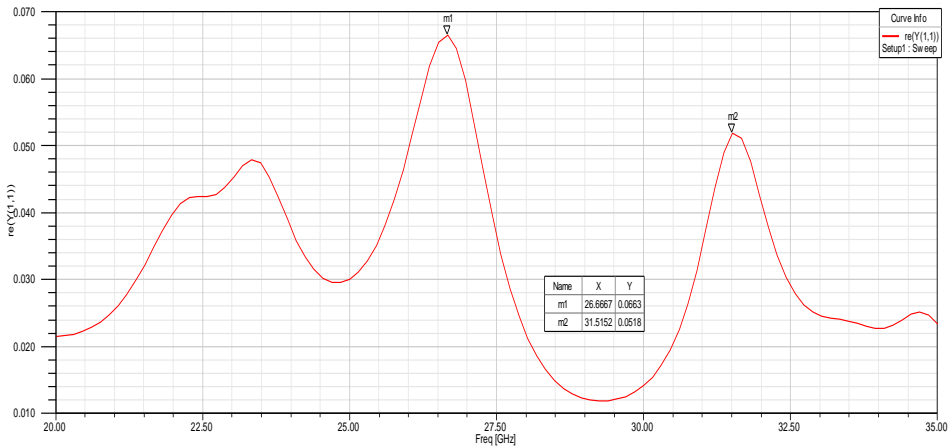


Fig. 7. Real Y-parameter.

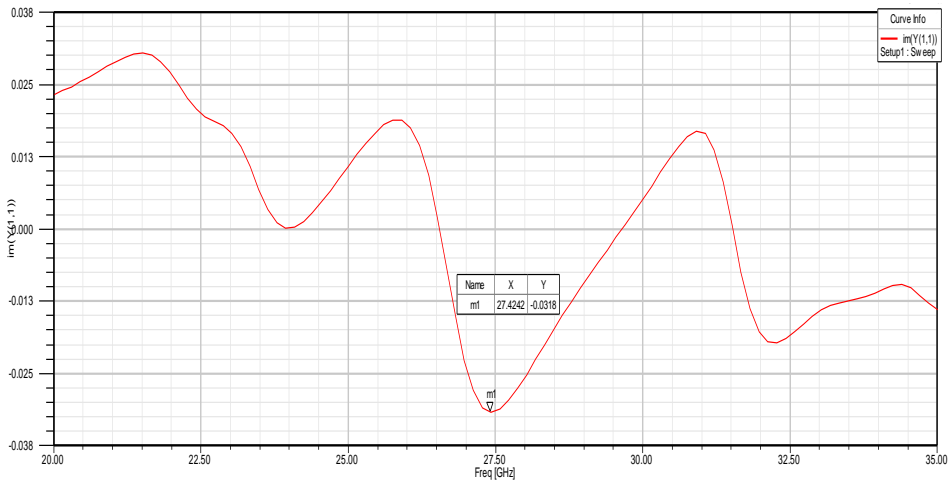


Fig. 8. Imaginary Y-parameter.

Directivity, expressed in dB, is the measure of the concentration of an antenna's radiation pattern in a particular direction. An antenna that radiated equally well in all directions would be omnidirectional and have a 1 (0 dB) directivity. The higher the directivity, the more concentrated or focused the beam radiated by an antenna. The simulation results of the antenna's directivity at the operational frequencies 24 and 29 GHz are 0.5385 and 0.8729 dB, respectively (Fig. 9).

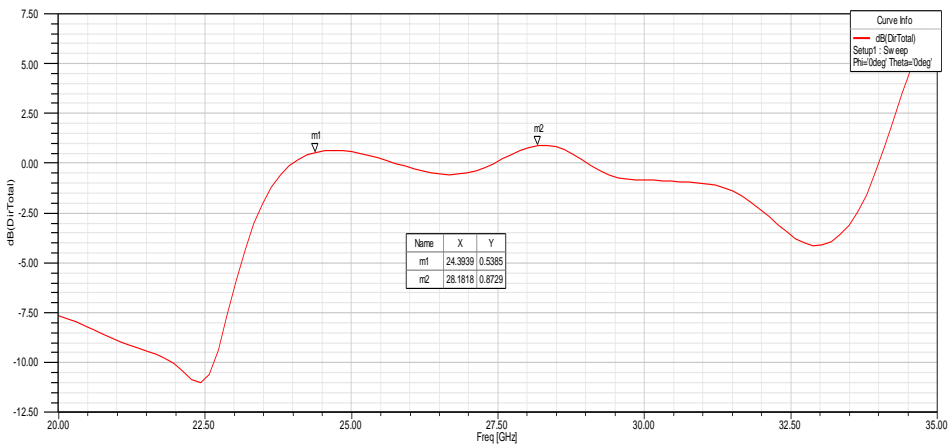


Fig. 9. Directivity versus frequency graph. Simulation results of directivity of the antenna at the operational frequencies 24 and 29 GHz are 0.5385 and 0.8729 dB, respectively.

3.2. Measured results

After HFSS design, the antenna is simulated and fabricated, and the result parameters are recorded for experimental validation. The antenna patch was calculated based on the

standard microstrip equation, and the dimension was adjusted for optimization. The antenna design with patch dimensions is mentioned in Fig. 10, and the prototype of the fabricated antenna consisting of four patches on the substrate along the middle mainline is shown in Fig. 11. The Mainline contact is 10.1 mm long and 1 mm thick. Rectangular patches from the bottom of the design are of lengths 8, 6, 4, and 3 mm and are written as $l_4, l_3, l_2,$ and l_1 . For the calculated patches, the width of each patch turns out to be 1.5 mm and is labeled as $b_4, b_3, b_2,$ and b_1 . The distance between the first two patches (a_2) is 1 mm, and between the second and third patches (a_3) is 2 mm. The third and fourth patches are again 1 mm apart (a_4). The substrate used is FR4 (dielectric constant 4.4) with a loss tangent of 0.0022. A microstrip line of width 1 mm for a 50Ω impedance line is used to match with the load antenna for supplying energy to the four radiating patches.

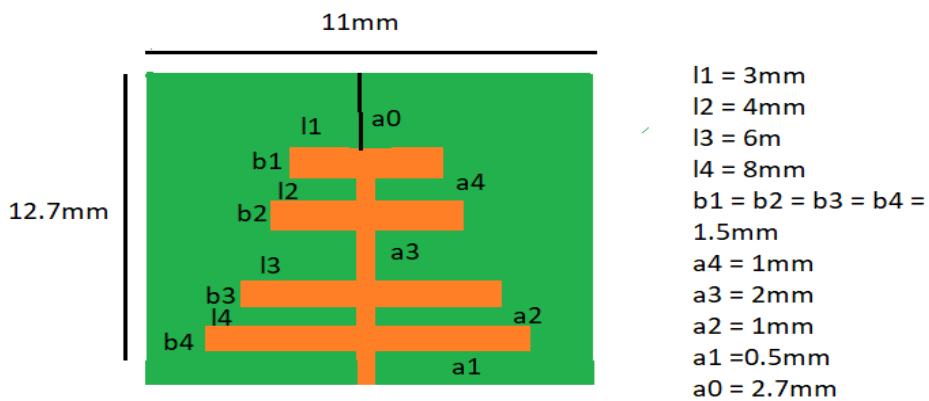


Fig. 10. Antenna design with dimensions in mm.



Fig. 11. Prototype of four-patch antenna.

The simulated and fabricated results are compared. The result parameters of the fabricated antenna are measured by a Voltage Network Analyzer (Fig. 12).



Fig. 12. Front view of Voltage Network Analyzer.

Measured values of S11 and VSWR plotted against frequencies are shown in Figs. 13 and 14, respectively. A comparison between the simulated and measured results is made in Table 3. Almost an exact match has been obtained between the simulated and measured results.

Table 3. Comparison between simulated and measured results.

Parameter	Result	24 GHz	29 GHz	34 GHz
S11(dB))	Simulated	-13.05	-13.15	-12.73
	Measured	-10.73	-14.35	-13.25
VSWR	Simulated	1.57	1.57	1.60
	Measured	1.48	1.60	1.48

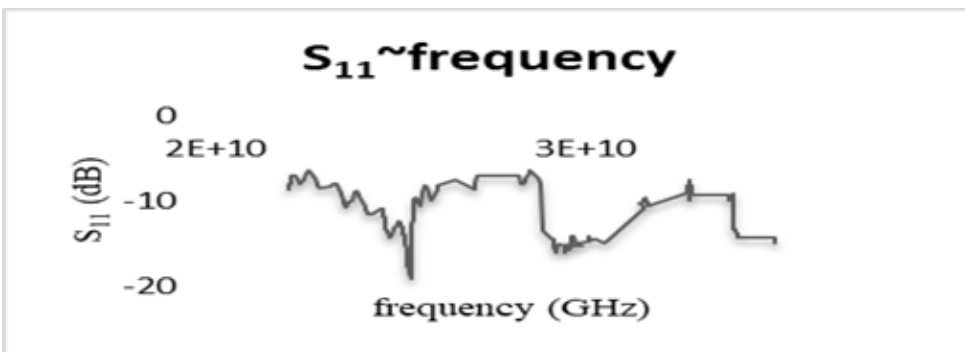


Fig. 13. Measured values of S11 due to fabricated antenna.

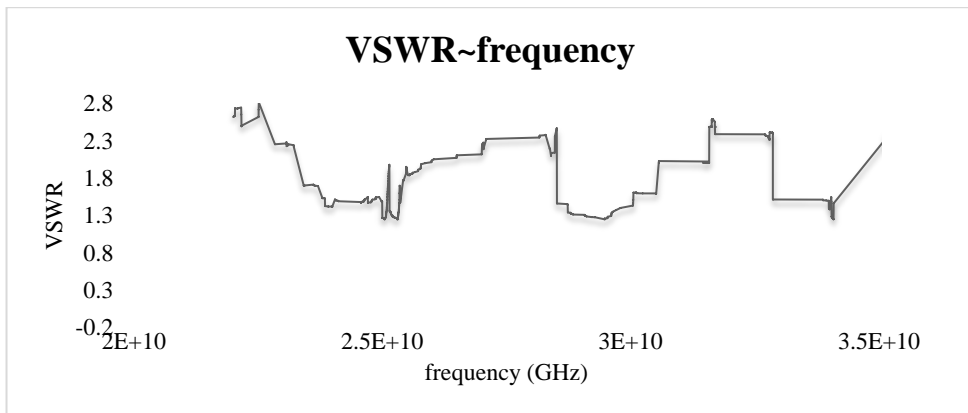


Fig. 14. Measured values of VSWR due to fabricated antenna.

A nearly perfect match between the simulation and measured results and their values being close to the 5G/6G mobile communication requirement qualifies the designed antenna for 5G/6G mobile communication application.

4. Conclusion

In this work, we have designed a compact and novel microstrip quad patch triple band Yadi-Uda alike antenna on the Ansys HFSS platform, on a volumetric dimension of $11 \times 12.7 \times 1.6 \text{ mm}^3$, suitable for new generation 5G/6G mobile communication. The radiating element is obtained with four different size rectangular patches of lengths 8, 6, 4, and 3 mm, each of width 1.5 mm, extending outward from the mainline metal strip of length 10.1 mm. Impedance matching of the antenna is done by tuning the size of patches in the feeding portion. A microstrip line of 50Ω impedance is used to match with the load antenna for supplying energy to the four radiating patches. The designed antenna is simulated, and its experimentation validation is successfully done regarding standard antenna parameters S11, VSWR, gain, etc. Against the 5G band gain requirement of 4.55 dBi, it has a comparatively good gain of 6.16 dBi. Return loss of value less than -10 dB with bandwidth ranging from 0.8 to 2 GHz is claimed around 24, 29, and 34 GHz resonant frequencies. A good agreement is found between the simulated and measured results, which makes it a suitable candidate for 5G/6G mobile communication applications.

Acknowledgment

The authors express their gratitude to A. Banerjee, Jadavpur University, and P. Pal, Head of Microline, India, Kolkata, for the fabrication work of the antenna prototype.

References

1. E. A. Kadir, S. M. Shamsuddin, E. S. T. A. Rahman, S. K. A. Rahim, and S. L. Rosa, *Int. J. Circuits Syst. Signal Process.* **8**, (2014).
2. J. M. Laheurte, Wiley-ISTE: (Hoboken, NJ, USA, **272**, 2012).
<https://doi.org/10.1002/9781118603437.ch9>
3. A. Nella and A.S. Gandhi, *Proc. of the 2017 Int. Conf. on Advances in Computing, Communications and Informatics (ICACCI)*, Udipi, India, 13–16 September, (2017).
<https://doi.org/10.1109/ICACCI.2017.8126165>
4. C. A. Balanis, *Antenna Theory: Analysis and Design* (John Wiley & Sons, New York, USA, 2005).
5. Y. Rhazi, O. E. Bakkali, S. Bri, M. A. Lafkih, Y. E. Mrabet *et al.*, *Int. Symp. on Advanced Electrical and Communication Technologies (ISAECT)*, (2018).
<https://doi.org/10.1109/ISAECT.2018.8618828>
6. K. K. Giri, R. K. Singh, and K. Mamta - *4th Int. Conf. on Recent Trends in Computer Science and Technology (ICRTCST)*, Jamshedpur, India, (2022).
<https://doi.org/10.1109/ICRTCST54752.2022.9782051>
7. K. K. Giri, R. K. Singh, and K. Mamta, *J. Sci. Res.* **14**, 2 (2022).
<https://doi.org/10.3329/jsr.v14i2.55209>
8. Y. Kim, H. Lee, P. Hwang, R. K. Patro, J. Lee, *et al.*, *IEEE J. Selected Topics Signal Process.* **10**, 3 (2020). <https://doi.org/10.2528/PIERL21120202>
9. A. L. Swindlehurst, E. Ayanoglu, P. Heydari, and F. Capolino, *IEEE Commun. Magaz.* **52**, (2014). <https://doi.org/10.1109/MCOM.2014.6894453>
10. E. L. Bengtsson, F. Rusek, S. Malkowsky, F. Tufvesson, P. C. Karlsson, and O. Edfors, *IEEE Access* **5** (2017). <https://doi.org/10.1109/TVT.2019.2949738>
11. M. Giordani, M. Marco, and M. Zorzi, *IEEE Commun. Magaz.* **54**, 11 (2016).
<https://doi.org/10.1109/MCOM.2016.7786102>
12. K. Mamta and R. K. Singh, *British J. Appl. Sci. Technol.* **19**, 5 (2017).
<https://doi.org/10.9734/BJAST>
13. B. H. Sun, S. G. Zhou, Y.F. Wei, and Q.-Z. Liu, *Prog. Electromagnetics Res.* **100**, 2010.
<https://doi.org/10.2528/PIER09111501>
14. R. Bayderkhani and H. R. Hassani, *Prog. Electromagnetics Res. B*, **17**, 153 (2009).
<https://doi.org/10.2528/PIERB09072502>
15. M. Bemani and S. Nikmehr, *Prog. Electromagnetics Res. B* **16**, 389 (2009).
<https://doi.org/10.2528/PIERB09053101>
16. K. Mamta, R. K. Singh, N. K. Sinha, and R. Keshri, *Lect. Notes Electr. Eng.* **476**, 79 (2018).
https://doi.org/10.1007/978-981-10-8234-4_8
17. R. Garg, *Microstrip Antenna Design Handbook* (Boston, Artech House, 2000).
18. J. G. Andrews, S. Buzzi, W. Choi, S. V. Hanly, A. Lozano *et al.*, *IEEE J. Selected Areas Commun.* **32**, 6 (2014). <https://doi.org/10.1109/JSAC.2014.2328098>
19. A. Mahabub, M. M. Rahman, M. Al-Amin, M. S. Rahman, M. M. Rana, *Open J. Antennas Propag.* **6**, 1 (2018). <https://doi.org/10.4236/ojapr.2018.61001>
20. Y. Rafsyam *et al.*, *Proc. National Seminar of Sci. Technol.* **1**, 1 (2014).
21. P. Sunthari and R. Veeramani - *1st Int. Conf. on Recent Advances in Aerospace Engineering (ICRAAE)*, (2017). https://doi.org/10.1007/978-981-16-0443-0_14
22. F. Yuli, *J. Teknologi Rekayasa*, **22**, 2 (2017).
23. X. Lin, B. Seet, F. Joseph, and E. Li, *IEEE Antennas Wirel. Propag. Lett.* **17**, 1281 (2018).
<https://doi.org/10.1109/LAWP.2018.2842109>
24. Y. Yashchyshyn, K. Derzakowski, G. Bogdan, K. Godziszewski, D. Nyzovets, *et al.*, *IEEE Antennas Wirel. Propag. Lett.* **17**, 225 (2018). <https://doi.org/10.1109/LAWP.2017.2781262>
25. M. Tang, T. Shi, and R. W. Ziolkowski, *IEEE Trans. Antennas Propag.* **65**, 61 (2017).
<https://doi.org/10.1109/TAP.2015.2503732>
26. N. Yoon and C. A. Seo, *J. Electromagn. Eng. Sci.* **17**, 133 (2017).

27. S. X. Ta, H. Choo, and I. Park, *IEEE Antennas Wirel. Propag. Lett.* **16**, 2183 (2017).
<https://doi.org/10.1109/LAWP.2017.2703850>
28. K. Mamta and R. K. Singh, *Int. J. Mag, IT Eng.* **4**, 137 (2019).
29. P. A. Dzagbletey, Y. Jung, *IEEE Antennas Wirel. Propag. Lett.* **17**, 780 (2018).
<https://doi.org/10.1109/LAWP.2018.2816258>
30. M. Khalily, R. Tafazoll, P. Xiao, and A. A. Kishk, *IEEE Trans. Antennas Propag.* **66**, 4641 (2018). <https://doi.org/10.1109/TAP.2018.2845451>
31. S. Zhu, H. Liu, Z. Chen, and P. A. Wen, *IEEE Antennas Wirel. Propag. Lett.* **17**, 776 (2018).
<https://doi.org/10.1109/LAWP.2018.2816038>